Geosci. Model Dev. Discuss., https://doi.org/10.5194/gmd-2018-22
Manuscript under review for journal Geosci. Model Dev.
Discussion started: 20 March 2018

Geoscientific Model Development Discussions
Open Access
EGU

Implementation of a simple thermodynamic sea ice scheme, SICE version 1.0-38h1, within the ALADIN-HIRLAM numerical weather prediction system version 38h1

Yurii Batrak[1], Ekaterina Kourzeneva[2], and Mariken Homleid[1]

[1]Development Centre for Weather Forecasting, Norwegian Meteorological Institute, Oslo, Norway
[2]Finnish Meteorological Institute, Helsinki, Finland

Correspondence to: Yurii Batrak (yurii.batrak@met.no)

Abstract. Sea ice is an important factor affecting weather regimes, especially in polar regions. A lack of its representation in numerical weather prediction (NWP) systems leads to large errors. For example, in the HARMONIE-AROME model configuration of the ALADIN-HIRLAM NWP system, the mean absolute error in 2 metre temperature reaches 1.5 °C after 15 forecast hours for Svalbard. A possible reason for that is that the sea ice properties are not reproduced correctly (there is no prognostic sea ice temperature in the model). Here, we develop a new SImple sea iCE scheme (SICE) and implement it into the ALADIN-HIRLAM NWP system in order to improve the quality of its forecasts in areas influenced by sea ice. General evaluation of the new parameterization is performed within HARMONIE-AROME by experiments covering the Svalbard and Gulf of Bothnia areas for a selected period in March – April 2013. It is found that using the SICE scheme improves the forecast, decreasing the value of the 2 metre temperature mean absolute error on average by 0.5 °C in areas that are influenced by sea ice. The new scheme is sensitive to the representation of the form drag: it may increase the 10 metre wind speed bias on average by 0.4 $\mathrm{m\,s^{-1}}$ when the form drag is not taken into account. Also, the modelling results are compared with the sea ice surface temperature observations from MODIS. The warm bias (of approximately 5 °C) of the new scheme is indicated for the areas of thick ice in the Arctic. Impacts of the SICE scheme on the modelling results and possibilities for future improvement of sea ice representation in the ALADIN-HIRLAM NWP system are discussed.

1 Introduction

Sea ice, permanent or seasonal, covers large areas of the ocean, especially in polar regions. Sea ice is a complex system with many important processes occurring. Being an interface between the atmosphere and the underlying medium, the sea ice surface temperature (in contrast to the sea surface temperature) has a noticeable diurnal cycle. Snow is accumulated on the ice and is accompanied by specific processes of snow-ice formation during the cold season, and by snow melt and the appearance of melt ponds during the warm season. Freezing of saline water results in brine droplets becoming trapped in the ice. This affects not only the ice thermal properties but also the ice structure, due to the slow movement of the trapped droplets towards the ice bottom and the formation of channels. Finally, the ice covered area is not a solid shield but a mixture of floes and polynyas that drift, being forced by the wind and ocean currents. Large scale ice covered areas strongly affect the properties of

Geosci. Model Dev. Discuss., https://doi.org/10.5194/gmd-2018-22
Manuscript under review for journal Geosci. Model Dev.
Discussion started: 20 March 2018

the atmospheric surface boundary layer over them. Night cooling of the ice surface may lead to a very stable boundary layer and limited turbulent exchange between the surface and the atmosphere. Over areas with a mixture of floes and polynyas, the form drag appears, which affects the turbulent fluxes. Thus, it is very important to reproduce the processes over the sea ice correctly in numerical weather prediction models.

Traditionally in NWP applications, simple parameterization schemes for sea ice are used. Information about the presence of sea ice cover is taken from observations (the analysis), and the sea ice thickness and sea ice temperature are modelled by a parameterization scheme. For parameterization of the sea ice in NWP, two main approaches currently exist: sea ice schemes based on the solution of the heat diffusion equation with several ice layers, but constant ice thickness (ECMWF, HIRLAM) (ECMWF, 2017; Unden et al., 2002); and bulk sea ice models with prognostic ice depth and an assumed linear or polynomial shape of the temperature profile in the ice (DWD) (Mironov et al., 2012; Mironov and Ritter, 2004; Mironow and Ritter, 2003). Snow on ice in these schemes is either not represented (ECMWF), or represented parametrically via changing the albedo from ice to snow during the melting period (DWD) (Mironov and Ritter, 2004). Simple sea ice schemes are used for operational forecasting. However, their performance has mainly been studied in general, with minor validations against observations and without comparisons with more advanced ice models.

For ice forecasting applications and research purposes, more advanced ice models have been developed, for example CICE (Hunke et al., 2015), GELATO (Mélia, 2002) and HIGHTSI (Cheng and Launiainen, 1998). They are applied in ocean modelling (e.g., Blockley et al., 2014; Dupont et al., 2015), and in coupled ocean-ice-atmosphere systems for research purposes and seasonal forecasting (Brassington et al., 2015; Lea et al., 2015; MacLachlan et al., 2015; Pellerin et al., 2004). However, they are rarely used in operational NWP. One exception is the UK Met Office Unified Model, but to our knowledge there are no publications about the details of coupling between the advanced sea ice model and the atmospheric model in this system. There are a number of reasons that advanced sea ice models are not widely used for operational NWP. Firstly, the advanced ice models are computationally expensive, representing in detail many processes that are important for the evolution of the sea ice itself, but of secondary importance for the description of ice-atmosphere interactions. Secondly, their robustness and numerical stability during coupling with atmospheric models needs more studies within a framework of short range operational NWP systems. Thirdly, they may require advanced methods of data assimilation for their initialization. In NWP research, in addition to coupled systems, advanced ice models may be used for the performance assessment of simple schemes.

Observations of the sea ice properties that are currently used in NWP are very limited. They mainly indicate only the presence of ice. One example is the sea ice concentration product provided by Ocean and Sea Ice Satellite Application Facility (OSI SAF) (Andersen et al., 2012; Breivik et al., 2001), which uses observations from passive microwave sensors. This product is in turn included in the Operational Sea surface Temperature and sea Ice Analysis product (OSTIA) (Stark et al., 2007; Donlon et al., 2012). For using the sea ice concentration data in an NWP system, they need to be projected onto an atmospheric model grid, which is usually done during the analysis step. Subsequently, the sea ice concentration is used to govern the sea surface schemes: for the ice-covered part of a grid box, a simple ice model runs, for the ice-free part, the sea surface temperature is kept constant. To our knowledge, no other observations of ice properties are used for assimilation in short range NWP systems, and very few of them are used for validation. In ocean modelling systems, sea ice concentration and sea ice drift data from

Geosci. Model Dev. Discuss., https://doi.org/10.5194/gmd-2018-22
Manuscript under review for journal Geosci. Model Dev.
Discussion started: 20 March 2018

different sources, including remote sensing from passive microwave and visible channels are used (see, for example, Posey et al., 2015; Sakov et al., 2012). Acquisition of the sea ice depth data from active remote sensing is being developed (Tilling et al., 2016), but the latency of these data is not yet acceptable for operational use in short range forecasting. However, these data also could serve as a source of information about sea ice properties for an NWP system.

In the ALADIN-HIRLAM NWP system both the sea surface temperature and the sea ice surface temperature are kept constant during the whole forecast. They are initialised from an external source (for example, from the global ECMWF model IFS) each forecast cycle. Over ice-covered and in ice-surrounded areas, this causes noticeable errors in near surface air temperature forecasts, especially for forecasts longer than 24 hours.

The main purpose of this study is the development of a simple parameterization scheme for sea ice for the ALADIN-HIRLAM NWP system. The scheme that was developed solves the heat diffusion equation on a vertical grid within a sea ice slab of constant thickness. This level of simplification was chosen as a first step. Prognostic sea ice thickness, which needs special attention during the initialization and analysis step, is considered for future developments. Technically, the new sea ice scheme is developed in the framework of the land and ocean surface modelling platform SURFEX (Masson et al., 2013), which is incorporated in the ALADIN-HIRLAM NWP system. In the sea ice scheme, provision is made to couple it with the snow scheme from SURFEX after Boone and Etchevers (2001). Also, in the case of fractional ice cover, the form drag caused by ice floating over the water surface is taken into account following Lüpkes et al. (2012).

The simple sea ice model (parameterization scheme) is checked for sanity and its performance is assessed through a comparison with the off-line sea ice model HIGHTSI (Cheng and Launiainen, 1998). HIGHTSI, although not containing the ice dynamics (unlike CICE and GELATO), reproduces the temperature profiles in the ice with a sufficient level of accuracy (Cheng et al., 2008) and needs a minimal amount of forcing data. The overall performance of the HARMONIE-AROME configuration of the ALADIN-HIRLAM NWP system with the new sea ice parameterization scheme is evaluated against temperature and wind measurements from coastal meteorological (SYNOP) stations and ice surface temperature observations from the Moderate Resolution Imaging Spectroradiometer (MODIS). The scheme results in an improvement of the forecast verification scores of the ALADIN-HIRLAM NWP system in coastal areas that are influenced by sea ice, but it overestimates the sea ice surface temperature in the Arctic, where the prescribed constant value of the ice thickness is too small. The experiments described in this paper, and the experience gained, will enable a better understanding of the forecast errors and uncertainties and provide an advancement in the description of the interactions between sea ice and the atmosphere in NWP.

The paper is organized as follows. In Section 2 the scheme description is given, which includes an overview of the physical equations. Numerical methods to solve the scheme equation are described in Appendix A. Section 3 addresses the performance of the new scheme evaluated by comparison with the thermodynamic sea ice model HIGHTSI, measurements from SYNOP stations and observations from MODIS. In the final section a short summary of the obtained results is given and the perspectives for further developments are discussed. Fortran source code of the SICE scheme version 1.0-38h1 is provided in the Supplement.

Geosci. Model Dev. Discuss., https://doi.org/10.5194/gmd-2018-22
Manuscript under review for journal Geosci. Model Dev.
Discussion started: 20 March 2018

Geoscientific Model Development Discussions

2 Description of the sea ice parameterization scheme

The purpose of the SImple sea iCE scheme (SICE, pronounced "ess ice"), which is developed for the parameterization of sea ice in NWP, is the prediction of the surface temperature of a thick layer of sea ice. The ice thickness is prescribed. No ice melting or ice formation processes are included and the heat flux from water to ice is neglected. Processes of snow-ice formation, which are discussed e.g. by Saloranta (2000), are not represented. The scheme describes only the processes in the ice slab, but it is designed so that it can be naturally coupled with a snow scheme that can provide the value of the heat flux on the lower boundary of the snow layer. The prognostic temperature profile in the ice is obtained from the solution of the heat diffusion equation using the heat balance equation and the temperature of water freezing as upper and lower boundary conditions respectively:

$$\begin{cases} C\frac{\partial T}{\partial t} = \frac{\partial}{\partial z}\lambda\frac{\partial T}{\partial z} - \frac{\partial Q}{\partial z} & \\ 0 = F + \lambda\left.\frac{\partial T}{\partial z}\right|_{z=0} & \text{if } z = 0, \\ T = T_{frz} & \text{if } z = H, \end{cases} \tag{1}$$

where t is time (s); z is depth (m); C is the volumetric heat capacity of ice ($\mathrm{W \cdot s\ m^{-3}K^{-1}}$); λ is the ice thermal conductivity ($\mathrm{W\ m^{-1}K^{-1}}$); Q is the solar radiation flux penetrating through the ice ($\mathrm{W\ m^{-2}}$); T is the ice temperature (K); T_{frz} is the freezing point of sea water (K); and H is the prescribed ice thickness (m). The term F in the second row of Eq. (1) represents the balance of incoming downward and upward heat fluxes:

$$F = \delta_{H_{snow}}\left(LW\downarrow - \varepsilon\sigma T_s^4 - \rho_a c_p c_{\mathrm{H}} V_{\mathrm{N}}\left(T_s - T_{\mathrm{N}}\right) - L\rho_a c_{\mathrm{H}} V_{\mathrm{N}}\left(q_{sat}(T_s) - q_{\mathrm{N}}\right)\right) + \left(1 - \delta_{H_{snow}}\right) G_{snow} \tag{2}$$

where $\delta_{H_{snow}}$ is the Kronecker delta:

$$\delta_{H_{snow}} = \begin{cases} 1 & \text{if } H_{snow} = 0, \\ 0 & \text{if } H_{snow} \neq 0; \end{cases} \tag{3}$$

and T_s is the ice surface temperature (K) ($T_s \equiv T|_{z=0}$); $LW\downarrow$ is the downward longwave radiation flux ($\mathrm{W\ m^{-2}}$); ε is the surface emissivity; σ is the Stefan-Boltzmann constant ($\mathrm{W\ m^{-2}K^{-4}}$); ρ_a is the air density ($\mathrm{kg\ m^{-3}}$); c_p is the air heat capacity with constant pressure ($\mathrm{W \cdot s\ kg^{-1}K^{-1}}$); c_{H} is the drag coefficient for heat; V_{N} is the wind speed ($\mathrm{m\ s^{-1}}$); T_{N} is the air temperature (K); L is the latent heat of sublimation ($\mathrm{W \cdot s\ kg^{-1}}$); $q_{sat}(T_s)$ is the saturation specific humidity near the ice surface ($\mathrm{kg\ kg^{-1}}$); q_{N} is the specific humidity of air ($\mathrm{kg\ kg^{-1}}$); G_{snow} is the heat flux from snow to ice ($\mathrm{W\ m^{-2}}$); and H_{snow} is the snow thickness (m). Index N denotes a variable at some level in the atmosphere (the lowest atmospheric model level if the scheme is included in an atmospheric model). The right hand side of Eq. (2) is the sum of the longwave part of the radiative balance $LW\downarrow - \varepsilon\sigma T_s^4$ and the turbulent fluxes of sensible $H = \rho_a c_p c_{\mathrm{H}} V_{\mathrm{N}}\left(T_s - T_{\mathrm{N}}\right)$ and latent $LE = L\rho_a c_{\mathrm{H}} V_{\mathrm{N}}\left(q_{sat}(T_s) - q_{\mathrm{N}}\right)$ heat in the case of bare ice, or the heat flux from snow to ice in the case when snow is present.

The term Q in the first row of Eq. (1) describes the heat flux from solar radiation penetrating into the ice pack. For calculation of this heat flux, the Bouguer-Lambert law is used, with an approximation of radiation absorption in the thin layer of the ice

Geosci. Model Dev. Discuss., https://doi.org/10.5194/gmd-2018-22
Manuscript under review for journal Geosci. Model Dev.
Discussion started: 20 March 2018

Geoscientific Model Development Discussions
Open Access
EGU

following Grenfell and Maykut (1977):

$$Q(z) = \delta_{H_{snow}}(1-\alpha)SW{\downarrow}\, i_0 \cdot e^{-k\cdot z} \tag{4}$$

where α is the ice albedo; $SW{\downarrow}$ is the downward solar radiation flux ($\mathrm{W\ m^{-2}}$); i_0 is the fraction of radiation penetrating through the thin layer of the ice and k is the extinction coefficient for the ice ($\mathrm{m^{-1}}$), which is parameterized according to values suggested by Grenfell and Maykut (1977). The value i_0 parameterizes the vertical inhomogeneity of the ice transparency. It is dependent on depth: it is equal to 1 in the uppermost 0.1 m layer of ice, and to 0.18 in the lower layers (Grenfell and Maykut, 1977). Note that in the case of snow on ice, the remaining solar radiation that was not absorbed during penetration through the snow pack is assumed to be completely absorbed by the underlying ice surface.

The main prognostic variable of the SICE scheme is the temperature of the ice. Other parameters are either physical constants or should be taken from the external forcing. For calculation of the ice thermal conductivity and heat capacity we used the following formulations, which represent their dependency on the ice temperature and salinity (Schwerdtfecer, 1963; Feltham et al., 2006; Sakatume and Seki, 1978):

$$C = C_0 - \frac{T_{mlt}(S) - T_{mlt}(0)}{\theta^2} L \tag{5}$$

$$\lambda = \lambda_{bi} - (\lambda_{bi} - \lambda_b)\frac{T_{mlt}(S) - T_{mlt}(0)}{\theta} \tag{6}$$

where, following Bailey et al. (2010):

$$T_{mlt}(S) = 273.15 - 0.0592S - 9.37\cdot 10^{-6}S^2 - 5.33\cdot 10^{-7}S^3$$

$$\lambda_{bi} = \frac{2\lambda_i + \lambda_a - 2V_a(\lambda_i - \lambda_a)}{2\lambda_i + \lambda_a + 2V_a(\lambda_i - \lambda_a)}\lambda_i$$

$$\lambda_i = 1.162\left(1.905 - 8.66\cdot 10^{-3}\theta + 2.97\cdot 10^{-5}\theta^2\right)$$

$$\lambda_b = 1.162\left(0.45 + 1.08\cdot 10^{-2}\theta + 5.04\cdot 10^{-5}\theta^2\right)$$

$$\lambda_a = 0.03 \qquad V_a = 0.025$$

and C_0 is the volumetric heat capacity of the fresh ice ($\mathrm{W\cdot s\ m^{-3}K^{-1}}$); $T_{mlt}(S)$ is a function of the melting point of the saline ice depending on the salinity (K); S is the ice salinity, parts per thousand; $\lambda_{\{i,b,bi,a\}}$ is the heat conductivity of fresh ice, brine, bubbly ice and air respectively ($\mathrm{W\ m^{-1}}$); V_a is the fractional volume of air in the sea ice; and θ is the ice temperature in °C.

In the case of bare ice (no snow), information about the ice albedo is needed to calculate the surface energy balance from Eq. (2). The ice albedo strongly affects the temperature regime of the ice pack. The effects of some processes taking place on the ice surface, such as the effect of melt ponds, may be parameterized through the ice albedo even without their real physical description. In the SICE scheme, we propose a choice between several options based on simple parameterizations of ice albedo from (Perovich, 1996; Parkinson and Washington, 1979; Roeckner et al., 1992). In these parameterizations, albedo is defined as a constant value or as a function of the ice surface temperature. Numerical methods to solve Eq. (1) and Eq. (2) are presented in Appendix A.

Geosci. Model Dev. Discuss., https://doi.org/10.5194/gmd-2018-22
Manuscript under review for journal Geosci. Model Dev.
Discussion started: 20 March 2018

Geoscientific Model Development Discussions
Open Access
EGU

The assumption of bare ice is the simplest possible approximation and may give reasonable results. However, such a simple parameterization would describe processes on the ice surface covered by snow in a very approximate way. Snow upon the ice serves as an insulating layer with higher albedo and lower thermal conductivity than the underlying ice, and for more physically correct simulations the ice scheme should reproduce the processes related to the evolution of snow on the ice surface. The form of the upper boundary condition presented by Eq. (1), which contains the heat flux from the snow layer to the ice layer F as a term, allows easy coupling with an external snow model to represent snow on ice. In our study, we used the snow module ISBA Explicit Snow (ISBA ES) (Boone and Etchevers, 2001; Boone, 2000) to represent processes in snow. In the current version of SICE, when snow pack exists, it always covers the ice part of the grid cell as a layer of uniform thickness.

ISBA ES is a multi-layer snow scheme with prognostic snow water equivalent, snow heat content and snow density. The number of layers may be defined by the user with a default value of 3. The uppermost snow layer is always less than or equal to 0.05 m. The scheme describes explicitly the following processes: snow accumulation due to precipitation, heat redistribution, melting processes and snow pack compaction. It also represents processes related to the melt water within a snow layer. The heat diffusion and surface energy balance equations are solved numerically with implicit schemes. The snow module needs information about the atmospheric forcing and the temperature, heat conductivity and thickness of the topmost layer of ice. It predicts the snow variables and also provides the flux from the snow pack to the underlying medium. Thus, the coupling between snow and ice schemes is explicit. The snow surface albedo in ISBA ES is calculated through a simple aging scheme, which covers dry- and wet-snow albedo degradation formulations. In this aging scheme, the snow albedo may decrease during the degradation process from its maximum value of 0.85 to a minimum value of 0.5. When applying this scheme over sea ice, a snow albedo minimum value of 0.75 is used following (Perovich, 1996; Semmler et al., 2012). The ISBA ES scheme was developed to parameterize snow over land surfaces, thus it contains no parameterizations of specific snow-over-ice processes, such as snow-ice formation or evolution of melt ponds.

For better representation of the surface processes, an atmospheric model may apply a tiling approach. This means that a model grid cell may be covered with a mixture of both sea water and ice. When a grid box contains a certain amount of ice and open water, the ice and open water calculations are performed independently and the output flux to the atmosphere is represented by a weighted average of the fluxes from the water and ice parts. In this case information about the ice concentration may be utilized to obtain the weighting coefficients. Ice concentration is estimated from satellite observations using the analysis procedure. This procedure contains a consistency check between the sea surface temperature and sea ice concentration fields (Stark et al., 2007; Donlon et al., 2012).

Turbulent exchange between the sea ice and the atmosphere is a complex process that is influenced by the morphological features of the ice pack such as the presence of melt ponds, ice topography, ridges and deformations. In the current version of the SICE scheme these complex features are not represented and the ice part of the grid cell is assumed to be a flat surface with uniform characteristics. When the sea ice concentration is less than 100 % (which means a mixture of open water and sea ice), one more factor influences the turbulent exchange with the atmosphere. This is the form drag, which is caused by the floes floating on the water with their upper edge higher than the water surface (ice obstacles). This subtle effect might be important for NWP because the ice concentration from observations is considered in NWP as a percentage of ice in a grid cell. Indeed, the

Geosci. Model Dev. Discuss., https://doi.org/10.5194/gmd-2018-22
Manuscript under review for journal Geosci. Model Dev.
Discussion started: 20 March 2018

roughness length of water is lower than that of ice, and simple weighted averaging according to the ice concentration values will lead to a decrease of the roughness length (compared to fully ice-covered area), while in nature it should increase. An accurate sea ice scheme should include a parameterization of the drag caused by ice obstacles (the form drag). Such schemes, discussed for example in Lüpkes et al. (2012), usually introduce an additional term in the weighted average, which depends on the ice fraction. The form drag was introduced into the SICE scheme in the following way:

$$C_{d,mean} = \eta C_{d,ice} + (1-\eta) C_{d,sea} + C_{d,f} \tag{7}$$

where $C_{d,\{ice,sea,mean\}}$ is the drag coefficient over ice, sea and the mean drag coefficient over the grid cell respectively, under neutral conditions; η is the fraction of sea ice in the grid cell; and $C_{d,f}$ is the form drag. For calculation of the form drag term a parameterization suggested by Lüpkes et al. (2012) was used:

$$C_{d,f} = 7.68 \cdot 10^{-3} \left[\frac{\ln(0.41/z_{0,w})}{\ln(10/z_{0,w})} \right]^2 (1-\eta)^{\beta} \eta \tag{8}$$

where $z_{0,w}$ is the roughness length of the sea water surface and β is the tuning constant. Parameters of the SICE scheme are summarized in Table 1.

Technically, the SICE scheme was developed as a part of the externalized land and ocean modelling platform SURFEX (Masson et al., 2013). The externalized surface modelling platform SURFEX is a set of models used for the description of different types of surfaces: sea and inland water bodies, soil/vegetation and urban environments. It assumes a tiling approach, distinguishing different surface types in one box of an atmospheric model grid. Each atmospheric model grid box contains some fraction of 4 different surface types (tiles): nature, urban, inland water and sea. Fractions of these tiles are actually model parameters, they are permanent and known from land-use maps. For land-use mapping (physiography) SURFEX incorporates the 1 km resolution database ECOCLIMAPII (Faroux et al., 2013). Over a sea tile, in turn, some fraction of sea ice may exist. This fraction is constant during the forecast run, but it changes at the moment of analysis (model initialization) according to the sea ice concentration estimated from observations. Thus, sea ice may be considered as sub-tile (or patch). The functionality of using main tiles is provided by SURFEX, but the possibility to use information about the fractional sea ice was introduced into SURFEX while implementing the SICE scheme. SICE utilizes the standard heat diffusion equation solver from the SURFEX suite. SICE, which will in future contain a more advanced description of the sea ice, provides technical compatibility with the developing versions of SURFEX. It is important to mention that SURFEX provides the possibility to diagnose screen level meteorological values (2 metre temperature and specific humidity and 10 metre wind speed) from the predicted surface state and the atmospheric values (provided that the forcing is given at some upper level or at the lowest level of the host model) using the interpolation-like procedure of Businger et al. (1971).

The modelling platform SURFEX is incorporated into the ALADIN-HIRLAM NWP system to parameterize the underlying surface processes. The ALADIN-HIRLAM NWP system includes the model configuration HARMONIE-AROME (Bengtsson et al., 2017), which is a version of the non-hydrostatic limited area atmospheric model AROME (Seity et al., 2011). A variety of sub-grid scale physical processes are taken into account by the model parametrization schemes. In the ALADIN-HIRLAM NWP system, boundary conditions and some initial conditions are taken from larger scale models, such as IFS (ECMWF) or

Geosci. Model Dev. Discuss., https://doi.org/10.5194/gmd-2018-22
Manuscript under review for journal Geosci. Model Dev.
Discussion started: 20 March 2018

Geoscientific Model Development Discussions
Open Access
EGU

HIRLAM. The ALADIN-HIRLAM NWP system contains a data assimilation system that uses the three-dimensional variational analysis (3DVAR) method for upper air. Data assimilation of the surface variables uses the optimal interpolation method for screen level temperature, relative humidity and snow depth. In the configuration of the system used in this study, variables in the soil are initialized according to the optimal interpolation method described in Mahfouf et al. (2009).

3 Performance of the sea ice parameterization scheme

The main objective of the simple sea ice parameterization scheme is to reproduce the evolution of ice surface temperature, since this variable provides an interface between the atmosphere and the underlying surface. Observations of sea ice surface temperature in the area of interest, which may be used to evaluate the performance of the model/parameterization scheme, are limited. For testing the SICE scheme as a part of the ALADIN-HIRLAM NWP system, we compared the modelling results with the screen-level atmospheric observations. Visual comparisons with sea ice surface temperature observations from MODIS were also performed. Before verification against observations, we compared modelling results from SICE with the results of the well tested sea ice model HIGHTSI (Cheng and Launiainen, 1998). The purpose of this comparison was the overall technical sanity check of SICE and better understanding of its limitations and weaknesses.

3.1 Preliminary experiments comparing SICE and HIGHTSI results

HIGHTSI is a one dimensional thermodynamic sea ice model, which was developed for research purposes and climate studies. The model describes the evolution of ice mass and energy balance and is based on the heat conduction equation, which is solved with an implicit finite difference numerical scheme (Launiainen and Cheng, 1998). Parameterization of snow in HIGHTSI includes processes of snow accumulation from the forcing precipitation, snow melting and refreezing, and snow-ice formation (which in our experiments was switched off). Comparison with HIGHTSI was carried out in off-line (stand-alone) mode, since HIGHTSI is not coupled with an atmospheric model.

For the atmospheric forcing we used data from HIRLAM (Unden et al., 2002) operational forecasts (with a horizontal spatial resolution of 8 km), namely: lowest model level air temperature, wind speed and specific humidity; surface pressure; global downward shortwave and downward longwave radiation fluxes at the surface; rainfall and snowfall rates. Stand-alone experiments were performed for the 12 selected synoptic stations in the Svalbard coastal area, see Fig. 1. The period of off-line experiments was from August 2011 to June 2012, with a temporal resolution of the forcing data of one hour. For each model, 2 experiments were performed: a snow-free experiment, and an experiment considering the evolution of snow. For ice albedo, a simple parameterization based on Roeckner et al. (1992) was used. The ice salinity was set to a uniform value of 3 ppt.

In the SICE scheme, the prescribed ice thickness was given a value of 0.75 m, with 4 layers in the ice slab and 3 layers within the snow. HIGHTSI was configured in the default way with 20 layers within the ice slab and 10 layers within the snow pack. The first month of the simulations was considered as a spin-up.

We analyse here the results of the experiments only for the period when the ice thickness modelled by HIGHTSI was approximately equal to the ice thickness prescribed in SICE. In this way we see the difference in reproducing the thermal

Geosci. Model Dev. Discuss., https://doi.org/10.5194/gmd-2018-22
Manuscript under review for journal Geosci. Model Dev.
Discussion started: 20 March 2018

regime in the ice between the two schemes. Here we consider "small" ice thickness difference between the two models to be less than 0.4 m. In "no-snow" experiments, the period of small ice thickness difference lasted approximately for 3 months, from mid-September to mid-December. "No-snow" experiments showed that SICE and HIGHTSI tend to produce similar results for the period of the small ice thickness difference. When the ice thicknesses are very different, the ice surface temperature values may differ by more than 5 °C. In the experiments with the snow schemes included, the evolution of the snow thickness was quite similar in HIGHTSI and SICE. Due to the presence of snow in these experiments, the ice thickness in HIGHTSI was lower, so that the period of small ice thickness difference lasted from mid-September to the end of June. When the ice surface is insulated by snow and only the thin snow layer reacts to the atmospheric forcing, the oscillations of the snow surface temperature are very large. Due to this high variability, the snow surface temperature was sometimes very different between the HIGHTSI and SICE experiments, with a maximum difference of 3–5 °C. In general, the mean value of the surface temperature difference between SICE and HIGHTSI for all 12 points in the "no-snow" experiments was 0.71 °C (SICE gave higher values than HIGHTSI), with a difference standard deviation of 1.04 °C. For "snow" experiments these values are -0.46 °C (SICE gave lower values than HIGHTSI), with a standard deviation of 1.99 °C.

From these preliminary experiments with stand-alone runs, we conclude that the SICE scheme is able to adequately reproduce the evolution of the ice surface temperature, but the result is sensitive to the value of the prescribed ice thickness. Thus, the ice thickness may be important even if the main focus of simulations is the ice surface temperature. However this approach with the prescribed ice thickness, although being very simplified, may reproduce the ice surface temperature oscillations of different time scales and serve as a first approximation for the description of the sea ice cover behaviour.

3.2 Experimental configuration of the ALADIN-HIRLAM NWP system

For coupled experiments, the HARMONIE-AROME model configuration (Bengtsson et al., 2017) of the ALADIN-HIRLAM NWP system was used. Prior to implementation of the SICE scheme into the ALADIN-HIRLAM NWP system (through SURFEX), sea ice was accounted for in a very crude way. The ice surface temperature was simply equal to its initial value through the whole forecasting period (similar to the sea surface temperature); this introduced large errors, mainly connected to the absence of a diurnal cycle over the ice surface. To produce forecasts, HARMONIE-AROME performs short-term cycles, each cycle contains the data assimilation procedure and the model forecast. The background for the data assimilation are fields of prognostic variables at the end of the previous model forecast. In the configuration of HARMONIE-AROME used in this study, the length of the cycle was 3 hours. Starting from 0000 UTC and 1200 UTC analysis times, longer forecasts (up to 48 hours) are performed. Each cycle, the sea water surface temperature and the fraction of sea ice are interpolated bilinearly from the host model IFS, with extrapolation by the nearest neighbour method in specific areas such as fjords. The same is done with the initial value of the sea ice surface temperature. In turn, IFS uses OSTIA data (Donlon et al., 2012) for the sea surface temperature and ice fraction. For the ice surface temperature, it runs its own simple ice model. Thus, without SICE, HARMONIE-AROME actually used the sea ice surface temperature values modelled by IFS.

If the SICE scheme is used, its prognostic variables are updated during each cycle as described in the following. If in the grid cell in question the ice cover exists in the background field, the prognostic variables of SICE are kept unchanged (SICE

Geosci. Model Dev. Discuss., https://doi.org/10.5194/gmd-2018-22
Manuscript under review for journal Geosci. Model Dev.
Discussion started: 20 March 2018

runs freely). Otherwise, in the situation when the new ice is observed according to OSTIA, the initial (analysed) values of the prognostic SICE variables are obtained via extrapolation from the nearest grid cells of the background field, where the ice exits. The fraction of sea ice is also interpolated (or extrapolated) from OSTIA.

For this study, HARMONIE-AROME experiments were performed over two operational domains (see Fig. 1): (A) the AROME Arctic domain, which includes large ice-covered areas in the Arctic ocean, and (B) the MetCoOp domain, where the ALADIN-HIRLAM NWP system with HARMONIE-AROME is run operationally in a cooperation between the Norwegian Meteorological Institute and the Swedish Meteorological and Hydrological Institute[1] (Müller et al., 2017), and which covers the Scandinavian peninsula and the Baltic sea. Grids over both domains have a horizontal spatial resolution of 2.5 km. Experiments cover the time period from March to April of 2013. Four experiments defined for this part of the study are summarized in Table 2. These are: the reference experiment (REF) without the SICE scheme, SICE experiments without and with the ISBA ES snow module (SICE2D-NS and SICE2D-S respectively), and a SICE experiment with the form drag parameterization included (SICE2D-AD). The following SICE configuration was used in the experiments: the prescribed thickness of the ice pack was given the value 0.75 m with 4 layers in the ice, the ice albedo was calculated based on Roeckner et al. (1992). For the SICE2D-AD experiment the coefficient β in Eq. (8) was set to a value of 1. The experiments SICE2D-S and SICE2D-AD were only run over the Arctic domain. In SICE2D-S, the default 3 layer configuration of the snow scheme was chosen. The SICE2D-S experiment started from the snow-free state and accumulated snow from the precipitation during the modelling period. The ice fraction was taken into account in all SICE experiments. The sea ice fraction was the only sea ice variable that was influenced by observations in the analysis procedure.

3.3 Experiments with the SICE scheme included in the ALADIN-HIRLAM NWP system: validation against meteorological observations

For the evaluation of the model performance, measurements from 12 Svalbard stations and 6 stations situated in the coastal area of the Gulf of Bothnia were used. These stations are strongly affected by the sea and may show the impact of the improved ice representation. Some Svalbard stations are located in fjord areas where the forecast is strongly dependent on the quality of the ice fraction field. Due to the low resolution of the original ice fraction data and a too crude extrapolation procedure, for some ice-covered fjords only open water existed in the model runs. Stations located in such fjords were excluded from the comparison.

Figures 2, 3 and 6 show the impact of the new sea ice scheme, including the representation of snow on ice and form drag. These figures show the statistics of the forecast errors obtained by sampling the forecasts starting from 0000 UTC during the period of the experiments for the selected points in the Svalbard and Bothnian areas. For the statistics, the mean forecast error (bias) and the forecast error standard deviation as a function of the forecast lead time for the mean sea level pressure, 2 metre temperature and 10 metre wind speed were calculated for various experiments. Note that statistics for REF and SICE2D-NS in Fig. 3 and Fig. 6 are different because they cover different time periods: the period of March-April of 2013 for Fig. 3 and the period of only March 2013 for Fig. 6.

[1]The Finnish Meteorological Institute joined the MetCoOp collaboration in September 2017 and MetCoOp domain was extended towards the east.

Geosci. Model Dev. Discuss., https://doi.org/10.5194/gmd-2018-22
Manuscript under review for journal Geosci. Model Dev.
Discussion started: 20 March 2018

Geoscientific Model Development Discussions

The main impact of the SICE scheme is seen in the scores for the 2 metre temperature. Figure 2b shows that in REF, over the Svalbard stations the 2 metre temperature forecasts have a negative bias increasing in absolute value with the forecast length from 0.5 °C up to 2 °C. This evolution is caused by the influence of the surface temperature over the sea (both the open water and ice cases), which remains constant during the whole forecast period in this experiment. For the Bothnian stations (see Fig. 3b and Fig. 3d) in REF, the 2 metre temperature mean error has a diurnal cycle. This is because the Bothnian stations are much more affected by the land than the Svalbard stations, and the underestimation of night-time 2 metre temperatures over land is a characteristic feature of the model known from operational verification (not shown). The situation is illustrated by Fig. 4, which represents the observed values of air temperature for Kemi I lighthouse (WMO No. 02863, station position: 65°25' N; 24°08' E) and the forecast time series of different length and starting time. It shows that for REF, the air temperature can be more than 5 °C lower in the model forecast than in reality.

The sea ice scheme allows the ice surface temperature to evolve in time and improves the 2 metre temperature forecasts. According to Fig. 2b, over Svalbard stations the 2 metre temperature bias for SICE2D-NS is smaller than for REF, it is now positive and has an almost constant value of 1 °C. For the Bothnian stations (see Fig. 3b and Fig. 3d) the bias in SICE2D-NS still has a diurnal cycle, but now the night-time errors are much smaller, only 1 °C in absolute value. The error standard deviation for the 2 metre temperature forecasts is also considerably smaller in SICE2D-NS compared to REF, especially for forecasts longer than 24 hours. For the Svalbard stations it is more than 4 °C in REF but only 3 °C in SICE2D-NS, and for the Bothnian stations these values are 3 °C and 2 °C (note that for the Bothnian stations the forecast error standard deviation also shows a diurnal cycle).

Although the mean sea level pressure is usually controlled by the large scale rather than local processes, a local positive impact for this field is also visible, especially for the Svalbard stations. Figure 2a shows that the mean sea level pressure positive bias of up to 0.5 hPa in REF is removed in SICE2D-NS. This happens due to warmer (in general) temperatures in SICE2D-NS. In terms of the mean sea level pressure error standard deviation there is no considerable difference between REF and SICE2D-NS for the Svalbard stations. For the Bothnian stations, there is no considerable difference between REF and SICE2D-NS experiments for both the mean error and error standard deviation of the mean sea level pressure.

For the 10 metre wind speed the experiment SICE2D-NS has an approximately 0.5 $\mathrm{m\,s^{-1}}$ higher mean error than REF for all forecast lengths. In REF, the 10 metre wind speed bias is positive, with a value between 0.1 and 0.5 $\mathrm{m\,s^{-1}}$, but in SICE2D-NS it is even larger (see Fig. 2c). The source of the increased wind speed is the absence of the form drag over fractional ice in SICE2D-NS. In REF the sea-related part of the grid cell may have only two states: either covered by open water or by ice. As a result, in this experiment all of the Svalbard stations are affected by the surrounding compact ice areas and the simulated wind speed at these points depends on the ice roughness length. In SICE2D-NS, the stations are surrounded by a mixture of ice and open water. In this case the average drag coefficient for momentum over the part of the grid cell related to the sea with ice is smaller than in REF, since the roughness of a water surface is much lower than that of ice. This leads to the higher wind speed values. Thus, this increased bias in SICE2D-NS is the effect of averaging the drag coefficients for the sea-related part of the grid cell between the drag coefficients over open water and ice. They are averaged with weights according to the ice fraction value and the form drag is not taken into account.

Geosci. Model Dev. Discuss., https://doi.org/10.5194/gmd-2018-22
Manuscript under review for journal Geosci. Model Dev.
Discussion started: 20 March 2018

In SICE2D-AD, the form drag is taken into account in the SICE scheme. In this experiment, we add the form drag only when calculating the momentum flux. The effect of the form drag term is shown in Fig. 5, displaying the difference between the drag coefficients calculated in an ordinary way and with the additional term. The impact of the form drag is mostly noticeable in areas near the ice edge, where the ice fraction field has values of around 60 %. This is in accordance with Elvidge et al. (2016); Tsamados et al. (2014); Lüpkes et al. (2012). In SICE2D-AD the wind speed bias is smaller than in SICE2D-NS and is just slightly larger than in REF, as shown in Fig. 6. This improvement is seen both for the Svalbard and Bothnian stations; for the Svalbard stations it is more pronounced, mainly due to the differences in the ice concentration fields around Svalbard and in the Baltic sea. The error statistics for the other fields are not deteriorated in SICE2D-AD compared to SICE2D-NS (not shown).

In the discussion above, we compared only the snow-free experiments, where the physical processes over ice are still represented very roughly. A more advanced modelling system should also simulate the snow layer on top of the ice pack. In SICE2D-S, the explicit snow scheme ISBA ES is used to represent the snow over ice. In terms of the 2 metre temperature errors, the results of SICE2D-S are worse than for SICE2D-NS, the bias in SICE2D-S for the Svalbard stations is almost the same as in REF (see Fig. 2). For the Bothnian stations, the bias in SICE2D-S is smaller than in REF, but still larger than in SICE2D-NS (see Fig. 3). Also, a shift in the bias diurnal cycle in SICE2D-S compared to SICE2D-NS can be seen. This shift is caused by the difference in the thermal resistances of the snow and ice in the SICE2D-S and SICE2D-NS experiments. The error standard deviation of the 2 metre temperature in SICE2D-S is also larger than in SICE2D-NS, but it is still smaller than in REF, both for the Svalbard and Bothnian stations, especially for longer lead times (see Fig. 2 and Fig. 3). These results are in accordance with the off-line experiments. These cold 2 metre temperatures in the SICE2D-S experiment may be caused by different reasons. When conditions in the atmospheric boundary layer are stable, the surface becomes decoupled from the atmosphere, and a positive feedback appears, which makes the surface temperature drop more and more. This situation is very difficult to reproduce in modelling. Moreover, model errors may be both positive or negative. This may depend on errors in boundary layer parameterization, radiation fluxes, snow density or precipitation. This complex problem is well explained e.g. in (Slater et al., 2001). In atmospheric modelling it is usually called “the stable boundary layer problem”, because it appears during the periods of low shortwave radiation, cooling surface and near-surface inversions. In Atlaskin and Vihma (2012) it is shown how this problem appears in different NWP systems. Also, errors in the amounts of snow accumulated by the model may affect the quality of the screen level temperature forecast. For example, a caveat of the current scheme is the absence of the snow-ice formation representation, which could be important in the case of a thick snow layer covering relatively thin ice. Parameterization of these effects would require description of the ice mass balance, which is not implemented in the current version of SICE. In addition, errors in the snow depth and snow water equivalent over the ice are not corrected by the snow data assimilation procedure, as happens over land.

Validation against coastal SYNOP observations allows the impact of the sea ice temperature evolution to understood on the local scale, which is the main concern of regional NWP models. However with observations from coastal stations only, we lack understanding of the ice temperature behaviour for larger scales.

Geosci. Model Dev. Discuss., https://doi.org/10.5194/gmd-2018-22
Manuscript under review for journal Geosci. Model Dev.
Discussion started: 20 March 2018

3.4 Comparisons with observations from MODIS

The purpose of the comparison with observations from MODIS was to assess the performance of SICE over large ice-covered areas, especially in the Arctic region. The satellite observations of sea ice surface temperature (Hall and Riggs, 2015a, b) were retrieved from the archives of the NASA Land Processes Distributed Active Archive Center (LP DAAC) for the thermal remote sensing sensor MODIS of the Terra satellite. The resolution of the data is approximately 1 km for swathe data and 4 km for daily fields. We used 5-minute images of different satellite swathes, attempting to consider the diurnal cycle of the sea ice surface temperature. Since the main focus was the large scale, we used a visual method for comparing maps. Statistical assessments require application of special methods, which were out of the scope of this study. Since MODIS observations use the optical band, they contain gaps due to cloudiness, which decrease the number of useful maps considerably.

First, we compared the results of model experiments described in Sec. 3.3 with MODIS data. During the period of these experiments (which is March-April 2013), the majority of satellite swathes within the area of interest providing the ice surface temperature data were day-time. Thus, from these data it was impossible to estimate the amplitude of the diurnal cycle of the ice surface temperature. In the model experiments, this amplitude in the polar Arctic regions was also not large during this period, approximately 8 °C for both the SICE2D-NS and SICE2D-S experiments. In the REF experiment, the diurnal cycle of the sea ice surface temperature was not reproduced within a single forecast because the ice temperature was prescribed. However, in general, the REF experiment in comparison with SICE2D-NS showed ice surface temperature values closer to those observed by MODIS for the first 24 hours of forecast. In the polar Arctic, the ice surface temperature simulated by SICE2D-NS was approximately 10 °C higher than observed by MODIS, while in REF is was only 5 °C higher. This happens because the ice model of IFS uses higher values for the prescribed ice thickness, namely 1.5 m (ECMWF, 2017) against 0.75 m in SICE. Note that IFS uses the parameter values to reproduce the large scale processes rather than local ones. Also, since the ice surface temperature derived from MODIS data corresponds to the clear-sky conditions, it tends to have cold bias in average scores comparing to in-situ measurements (see, e.g., Hall et al., 2004). For the SICE2D-S experiment, the results were closer to MODIS observations and to REF, which is in accordance with the point comparisons of Sec. 3.3. However, this may be the result of compensating errors.

Then, we compared MODIS observations with results of operational runs. SICE has been running operationally within the ALADIN-HIRLAM NWP system version 38h1.2 by Norwegian Meteorological Institute for the AROME-Arctic domain (Müller et al., 2017) since the end of October 2015 (in June 2017 the operational system was updated to the ALADIN-HIRLAM NWP system version 40h1.1). In the operational runs, the snow block in SICE is not active, and the prescribed value of the ice thickness is equal to 0.75 m, with 4 layers in the ice slab. Examples of the maps for 1 March 2017 and 9 March 2017 are given in Fig. 7. Here for the comparison we used the aggregated product of the sea ice surface temperature observations from all MODIS swathes per day (Hall and Riggs, 2015b) and daily average of the atmospheric model underlying surface temperature. From this figure, the simulated ice surface temperature is generally overestimated in comparison with the MODIS data for approximately 5 °C. This happens because of the too low value of the prescribed ice thickness in SICE. However, the surface temperature field patterns are reproduced well, see for example the narrow stripe of colder ice surface temperatures

Geosci. Model Dev. Discuss., https://doi.org/10.5194/gmd-2018-22
Manuscript under review for journal Geosci. Model Dev.
Discussion started: 20 March 2018

to the North-West of Svalbard on 01 March 2017. Overestimation of the ice surface temperature over large territories may deteriorate the large scale dynamic simulations in the operational forecast. However, in regional modelling the large scale dynamics are mainly governed by the boundary conditions from a global model thus less influenced by inaccuracies in the representation of the ice surface temperature. For this reason, we keep the prescribed sea ice thickness value in SICE optimized from comparisons with SYNOP observations (0.75 m) and do not increase it.

4 Conclusions

A simple thermodynamic sea ice scheme, SICE, to represent sea ice processes in NWP was developed. In this scheme, the temperature profile in the ice is predicted by solving the heat diffusion equation in the slab of ice with a prescribed thickness. The scheme design allows coupling with a snow scheme explicitly, via the fluxes and temperature at the snow-ice interface. Also, the scheme includes the form drag for the momentum flux in the surface layer due to ice obstacles in the case of the fractional ice cover.

The scheme was preliminarily tested by comparing it with the sea ice model HIGHTSI (Cheng and Launiainen, 1998) in off-line mode. In the off-line experiments, when the snow block was switched off in both schemes, the difference in the simulated ice surface temperature between SICE and HIGHTSI was small (the difference standard deviation is equal to 1.04 °C), when the ice thickness modelled by HIGHTSI was approximately equal to that prescribed in SICE. With the snow block included, due to high variability of the snow surface temperature, the difference between the two schemes was larger, with the difference standard deviation of 1.99 °C. From this comparison, the conclusion about overall sanity of SICE was made, but the sensitivity of the results to the prescribed value of the ice thickness was noticed.

General evaluation of SICE was performed in the coupled mode, within the HARMONIE-AROME configuration of the ALADIN-HIRLAM NWP system, to assess the scheme performance and to study possible errors. The ice fraction field for the SICE experiments was provided by the OSTIA product (Stark et al., 2007) via the lower boundary conditions from the ECMWF model, IFS. In the reference experiment, the sea ice surface temperature was taken from the IFS model and remained constant during the forecasting cycle. Coupled experiments were performed for the SICE scheme with and without the snow scheme and the form drag included. For validation, data from coastal SYNOP stations in the Svalbard and Gulf of Bothnia regions were used. Also, visual comparisons with observations from MODIS were performed.

In verification against measurements from coastal SYNOP stations, coupled experiments showed that the impact of SICE on the 2 metre temperature scores was positive without snow model, however with the snow model no clear positive impact was seen. For the mean sea level pressure verification scores, a minor positive impact was seen for all SICE experiments. In the SICE experiments without the form drag compared to the reference experiment (which contains no ice fraction representation), an increased positive 10 metre wind speed bias was noted. This bias was reduced due to accounting for the form drag in SICE. However our conclusion about the impact of the form drag is still preliminary, operational implementation will need additional testing, including experiments covering different seasons and tuning. Also, the form drag term strongly depends on the ice fraction value, thus ice concentration observations of better quality than low resolution passive-microwave data used in OSTIA

are desirable. For example, in Posey et al. (2015) it is shown that using high resolution passive-microwave data from Advanced Microwave Scanning Radiometer 2 (AMSR-2) leads to a substantial decrease in model errors.

Comparisons of the model experiments with observations from MODIS over the Arctic domain showed that the reference experiment simulated the ice surface temperature field with smaller bias than the SICE experiment (with no snow scheme included). This happens because the prescribed ice thickness in the simple ice model of IFS is tuned to reproduce the large scale fields rather than local effects, and it is larger than in SICE. However general patterns of the ice surface temperature field are well captured by SICE.

Our general conclusion from the numerical experiments is that SICE can improve forecasts of the HARMONIE-AROME configuration of the ALADIN-HIRLAM NWP system in ice-surrounded areas. At the moment we recommend to use it without snow parameterization for a trouble-proof result. The prescribed ice thickness is an important parameter, and since no estimates of the ice thickness from observations or other sources are used in the current version of ALADIN-HIRLAM NWP system, it should be tuned.

The simplest way to go forward is to replace the prescribed constant value of the ice thickness by the climatology, to reproduce its seasonal and horizontal large scale variations. Of course, in the future the scheme itself should reproduce the spatial and temporal inhomogeneity of the ice thickness. Further development will be focused on the physical processes that control the evolution of sea ice, such as ice freezing and melting. Additionally, possibilities to improve the parameterization of snow on sea ice will be studied. More tests on the parameterization of form drag are planned. The performance of the scheme will be evaluated for more regions and more seasons, for example for a summer period in the Arctic region when ice melting processes occur, which did not get much attention during this study. Melt ponds affect the atmosphere mainly through changing radiation fluxes, but they may also influence the modelling results of a whole NWP system, since they lead to higher uncertainty in the ice concentration observations coming from passive microwave remote sensing. The initialization of the ice parameterization scheme and model error corrections (especially for the snow module) using observations are also of high importance. The possibilities to use more observations and to develop methods to assimilate them, as well as to improve the methods of using existing observations, should be carefully studied.

Code availability. SICE is a part of the ALADIN-HIRLAM NWP system, which is not available for general public. A copy of the ALADIN-HIRLAM NWP system source code can be obtained, for non-commercial research purposes only, from a member institution of ALADIN or HIRLAM consortium in applicant's country after signing a standardized License Agreement. An extract from the source code of the ALADIN-HIRLAM NWP system version 38h1 that contains only the source code of the SICE scheme version 1.0-38h1 is available in the Supplement.

Geosci. Model Dev. Discuss., https://doi.org/10.5194/gmd-2018-22
Manuscript under review for journal Geosci. Model Dev.
Discussion started: 20 March 2018

Geoscientific Model Development Discussions

Appendix A: Numerical solution

To solve equations Eq. (1) and Eq. (2) numerically, the ice slab of thickness H is divided into K layers of equal thickness, except for the topmost layer. For the thickness of the topmost layer, the following formulation is used:

$$z_1 = min\left|z^*, \frac{H - z^*}{K-1}\right| \tag{A1}$$

$$z^* = \begin{cases} 0.05 & \text{if } H \geq 0.2 \\ 0.25 \cdot H & \text{otherwise} \end{cases} \tag{A2}$$

The ice temperature and thermal properties are assumed to be constant within the current layer. Then, according to the implicit Euler numerical scheme, the first row of Eq. (1) may be rewritten for the layer number $j = 1 \ldots K$ as follows (subscripts denote the layer number j, superscripts $^-$ and $^+$ denote the variables at the beginning and at the end of the time step Δt, Δz_j is the thickness of layer j)

$$\frac{C_j \Delta z_j}{\Delta t}\left(T_j^+ - T_j^-\right) = \frac{\bar{\lambda}_{j-1}}{\Delta \bar{z}_{j-1}}\left(T_{j-1}^+ - T_j^+\right) - \frac{\bar{\lambda}_j}{\Delta \bar{z}_j}\left(T_j^+ - T_{j+1}^+\right) - Q\big|_{z=z_j}^- + Q\big|_{z=z_j-\Delta z_j}^- \tag{A3}$$

where

$$\Delta \bar{z}_j = \frac{\Delta z_j + \Delta z_{j+1}}{2} \quad \text{and} \quad \bar{\lambda}_j = \frac{\Delta z_j \lambda_j + \Delta z_{j+1}\lambda_{j+1}}{\Delta z_j + \Delta z_{j+1}} \tag{A4}$$

This defines a tridiagonal matrix (see Boone (2000) for a detailed description). The skin temperature of ice could be obtained by integrating the first row of Eq. (1) over the topmost layer assuming that the properties of ice are constant within the selected layer. Thus, combined with the second equation from the system Eq. (1), Eq. (2) and Eq. (4), the equation for the ice temperature within the skin layer can be written as:

$$C_t \frac{\partial T_s}{\partial t} = \delta_{H_{snow}}(R_n - H - LE) + (1 - \delta_{H_{snow}})G_{snow} + \lambda \left.\frac{\partial T}{\partial z}\right|_{z=z_1} \tag{A5}$$

where $C_t \equiv C|_{z=z_1} \cdot \Delta z_1$ is the surface thermal resistance ($\mathrm{W \cdot s\ m^{-2}K^{-1}}$); Δz_1 is the thickness of the upper layer of ice (m); $R_n = (1 - i_0 \cdot e^{-k \cdot z_1})(1-\alpha)SW\downarrow + LW\downarrow - \varepsilon\sigma T_s^4$ is the radiative balance. The finite differential representation of Eq. (A5) with the implicit Euler scheme gives the upper row of the matrix Eq. (A3). In the case of no snow it reads:

$$\frac{C_t}{\Delta t}\left(T_s^+ - T_s^-\right) = R_n^\pm - H^\pm - LE^\pm - \frac{\lambda}{\Delta \bar{z}_1}\left(T_s^+ - T_1^+\right), \tag{A6}$$

Note that all the fluxes $R_n^\pm$, $H^\pm$, $LE^\pm$ are calculated using the prognostic variables at the end of the time step. For example, in the case of coupling with an atmospheric model, $H^\pm$ can be written as

$$H^\pm = \rho_a^- c_p^- c_{\mathrm{H}}^- V_{\mathrm{N}}^- \left(T_s^+ - T_{\mathrm{N}}^+\right) \tag{A7}$$

For obtaining the future value of T_{N}^+, a procedure known as "implicit coupling" (Best et al., 2004) is used. According to this procedure, the atmospheric variable X_N^+ from the lowest model level at the end of the time step can be found from

$$X_N^+ = A_{X,N}^- \cdot F_{X,S}^\pm + B_{X,N}^- \tag{A8}$$

Geosci. Model Dev. Discuss., https://doi.org/10.5194/gmd-2018-22
Manuscript under review for journal Geosci. Model Dev.
Discussion started: 20 March 2018

Geoscientific Model Development Discussions
Open Access
EGU

This procedure uses the coefficients $A^{-}_{X,N}$ and $B^{-}_{X,N}$ from the implicit numerical solution of the vertical diffusion scheme from the atmospheric model, and the surface flux $F^{\pm}_{X,S}$ of the variable X. The coupling coefficients in Eq. (A8) are provided by the host model. Term R_n in Eq. (A6) represents the radiative balance and contains the nonlinear term $\varepsilon\sigma {T_s^+}^4$, which defines the thermal radiation flux from the ice surface to the atmosphere at time step $t + \Delta t$. Linearization of this term can be done by use of the Taylor series which results in:

$$\varepsilon\sigma {T_s^+}^4 \approx 4\varepsilon\sigma {T_s^-}^3 T_s^+ - 3\varepsilon\sigma {T_s^-}^4 \tag{A9}$$

Then, Eq. (A8) and Eq. (A9) may be applied to transform Eq. (A6) to the form: $T_s^+ - \mathcal{A}_2 T_1^+ = \mathcal{A}_1$. This form is suitable to be the upper row in the tridiagonal matrix represented by Eq. (A3). For the lower boundary condition, the temperature at the bottom of the ice slab (at the bottom of the layer K) is equal to the freezing point of the sea water, according to the last equation of system Eq. (1). In this case, the lower row of the matrix represented by Eq. (A3) can be written as:

$$-\frac{\bar{\lambda}_{\mathrm{K}-1}}{\Delta\bar{z}_{\mathrm{K}-1}} T^+_{\mathrm{K}-1} + \left[\frac{C_{\mathrm{K}}\Delta z_{\mathrm{K}}}{\Delta t} + \frac{\bar{\lambda}_{\mathrm{K}-1}}{\Delta\bar{z}_{\mathrm{K}-1}} + \frac{2\bar{\lambda}_{\mathrm{K}}}{\Delta z_{\mathrm{K}}}\right] T^+_{\mathrm{K}} = \frac{C_{\mathrm{K}}\Delta z_{\mathrm{K}}}{\Delta t} T^-_{\mathrm{K}} + \frac{2\bar{\lambda}_{\mathrm{K}}}{\Delta z_{\mathrm{K}}} T_{frz} - Q\big|^-_{z=H} + Q\big|^-_{z=H-\Delta z_{\mathrm{K}}} \tag{A10}$$

The resulting system of linear equations may be solved through the Thomas algorithm (Thomas, 1949).

Actual implementation can be found in the source file `src/surfex/SURFEX/simple_ice.F90` available in the Supplement.

Competing interests. The authors declare that they have no conflict of interests.

Acknowledgements. The authors would like to thank Bin Cheng, Andrew Singleton and Laura Rontu for their constructive comments.

References

Andersen, S., Breivik, L.-A., Eastwood, S., Godøy, Ø., Lavergne, T., Lind, M., Porcires, M., Schyberg, H., and Tonboe, R.: Sea Ice Product Manual, Tech. rep., http://osisaf.met.no/docs/osisaf_ss2_pum_ice-conc-edge-type_v3p8.pdf, 2012.

Atlaskin, E. and Vihma, T.: Evaluation of NWP results for wintertime nocturnal boundary-layer temperatures over Europe and Finland, Quarterly Journal of the Royal Meteorological Society, 138, 1440–1451, https://doi.org/10.1002/qj.1885, http://dx.doi.org/10.1002/qj.1885, 2012.

Bailey, E., Feltham, D. L., and Sammonds, P. R.: A model for the consolidation of rafted sea ice, Journal of Geophysical Research: Oceans, 115, https://doi.org/10.1029/2008JC005103, http://dx.doi.org/10.1029/2008JC005103, c04015, 2010.

Bengtsson, L., Andrae, U., Aspelien, T., Batrak, Y., Calvo, J., de Rooy, W., Gleeson, E., Hansen-Sass, B., Homleid, M., Hortal, M., Ivarsson, K.-I., Lenderink, G., Niemelä, S., Nielsen, K. P., Onvlee, J., Rontu, L., Samuelsson, P., Muñoz, D. S., Subias, A., Tijm, S., Toll, V., Yang, X., and Køltzow, M. Ø.: The HARMONIE–AROME Model Configuration in the ALADIN–HIRLAM NWP System, Monthly Weather Review, 145, 1919–1935, https://doi.org/10.1175/MWR-D-16-0417.1, http://dx.doi.org/10.1175/MWR-D-16-0417.1, 2017.

Best, M. J., Beljaars, A., Polcher, J., and Viterbo, P.: A Proposed Structure for Coupling Tiled Surfaces with the Planetary Boundary Layer, Journal of Hydrometeorology, 5, 1271–1278, https://doi.org/10.1175/JHM-382.1, http://dx.doi.org/10.1175/JHM-382.1, 2004.

Blockley, E. W., Martin, M. J., McLaren, A. J., Ryan, A. G., Waters, J., Lea, D. J., Mirouze, I., Peterson, K. A., Sellar, A., and Storkey, D.: Recent developments of the Met Office operational forecasting system: an overview and assessment of the new Global FOAM forecasts, Geoscientific Model Development, 7, 2613–2638, https://doi.org/10.5194/gmd-7-2613-2014, 2014.

Boone, A.: Modeling hydrological processes in the land surface scheme ISBA: inclusion of a hydrological reservoir, ice and a snow model, Ph.D. thesis, Paul Sabatier University, 2000.

Boone, A. and Etchevers, P.: An Intercomparison of Three Snow Schemes of Varying Complexity Coupled to the Same Land Surface Model: Local-Scale Evaluation at an Alpine Site, Journal of Hydrometeorology, 2, 374–394, https://doi.org/10.1175/1525-7541(2001)002⟨0374:AIOTSS⟩2.0.CO;2, http://dx.doi.org/10.1175/1525-7541(2001)002<0374:AIOTSS>2.0.CO;2, 2001.

Brassington, G. B., Martin, M. G., Tolman, H. L., Akella, S., Balmeseda, M., Chambers, C. R. S., Chassignet, E., Cummings, J. A., Drillet, Y., Jansen, P. A. E. M., Laloyaux, P., Lea, D., Mehra, A., Mirouze, I., Ritchie, H., Samson, G., Sandery, P. A., Smith, G. C., Suarez, M., and Todling, R.: Progress and challenges in short- to medium-range coupled prediction, Journal of Operational Oceanography, 8, 239–258, https://doi.org/10.1080/1755876X.2015.1049875, 2015.

Breivik, L.-A., Eastwood, S., Godøy, Ø., Schyberg, H., Andersen, S., and Tonboe, R.: Sea ice products for EUMETSAT satellite application facility, Canadian Journal of Remote Sensing, 27(5), 403–410, https://doi.org/10.1080/07038992.2001.10854883, 2001.

Businger, J. A., Wyngaard, J. C., Izumi, Y., and Bradley, E. F.: Flux-Profile Relationships in the Atmospheric Surface Layer, Journal of the Atmospheric Sciences, 28, 181–189, https://doi.org/10.1175/1520-0469(1971)028⟨0181:FPRITA⟩2.0.CO;2, http://dx.doi.org/10.1175/1520-0469(1971)028<0181:FPRITA>2.0.CO;2, 1971.

Cheng, B. and Launiainen, J.: A one-dimensional thermodynamic air-ice-water model: technical and algorithm description report, MERI – Report Series of the Finnish Institute of Marine Research, 37, 15–36, 1998.

Cheng, B., Zhang, Z., Vihma, T., Johansson, M., Bian, L., Li, Z., and Wu, H.: Model experiments on snow and ice thermodynamics in the Arctic Ocean with CHINARE 2003 data, Journal of Geophysical Research: Oceans, 113, https://doi.org/10.1029/2007JC004654, http://dx.doi.org/10.1029/2007JC004654, c09020, 2008.

Donlon, C. J., Martin, M., Stark, J., Roberts-Jones, J., Fiedler, E., and Wimmer, W.: The Operational Sea Surface Temperature and Sea Ice Analysis (OSTIA) system, Remote Sensing of Environment, 116, 140–158, https://doi.org/10.1016/j.rse.2010.10.017, 2012.

Dupont, F., Higginson, S., Bourdallé-Badie, R., Lu, Y., Roy, F., Smith, G. C., Lemieux, J.-F., Garric, G., and Davidson, F.: A high-resolution ocean and sea-ice modelling system for the Arctic and North Atlantic oceans, Geoscientific Model Development, 8, 1577–1594, https://doi.org/10.5194/gmd-8-1577-2015, 2015.

ECMWF: PART IV: PHYSICAL PROCESSES, IFS Documentation, ECMWF, 2017.

Elvidge, A. D., Renfrew, I. A., Weiss, A. I., Brooks, I. M., Lachlan-Cope, T. A., and King, J. C.: Observations of surface momentum exchange over the marginal ice zone and recommendations for its parametrisation, Atmospheric Chemistry and Physics, 16, 1545–1563, https://doi.org/10.5194/acp-16-1545-2016, 2016.

Faroux, S., Kaptué Tchuenté, A. T., Roujean, J.-L., Masson, V., Martin, E., and P., L. M.: ECOCLIMAP-II/Europe: a twofold database of ecosystems and surface parameters at 1km resolution based on satellite information for use in land surface, meteorological and climate models, Geoscientific Model Development, 6, 563–582, https://doi.org/10.5194/gmd-6-563-2013, 2013.

Feltham, D. L., Untersteiner, N., Wettlaufer, J. S., and Worster, M. G.: Sea ice is a mushy layer, Geophysical Research Letters, 33, https://doi.org/10.1029/2006GL026290, http://dx.doi.org/10.1029/2006GL026290, 2006.

Grenfell, T. G. and Maykut, G. A.: The optical properties of ice and snow in the arctic basin, Journal of Glaciology, 18, 445–463, 1977.

Hall, D. K. and Riggs, G.: MODIS/Terra Sea Ice Extent 5-Min L2 Swath 1km, Version 6. Boulder, Colorado USA. NASA National Snow and Ice Data Center Distributed Active Archive Center, http://dx.doi.org/10.5067/MODIS/MOD29.006, 2015a.

Hall, D. K. and Riggs, G.: MODIS/Terra Sea Ice Extent and IST Daily L3 Global 4km EASE-Grid Day, Version 6. NASA National Snow and Ice Data Center Distributed Active Archive Center, http://dx.doi.org/10.5067/MODIS/MOD29.006, 2015b.

Hall, D. K., Key, J. R., Casey, K. A., Riggs, G. A., and Cavalieri, D. J.: Sea ice surface temperature product from MODIS, IEEE Transactions on Geoscience and Remote Sensing, 42, 1076–1087, https://doi.org/10.1109/TGRS.2004.825587, 2004.

Hunke, E. C., Lipscomb, W. H., Turner, A. K., Jeffery, N., and Elliott, S.: CICE: the Los Alamos Sea Ice Model Documentation and Software User's Manual, Tech. rep., Los Alamos National Laboratory, Los Alamos NM 87545, 2015.

Launiainen, J. and Cheng, B.: Modelling of ice thermodynamics in natural water bodies, Cold Regions Science and Technology, 27, 153 – 178, https://doi.org/http://dx.doi.org/10.1016/S0165-232X(98)00009-3, http://www.sciencedirect.com/science/article/pii/S0165232X98000093, 1998.

Lea, D. J., Mirouze, I., Martin, M. G., King, R. R., Hines, A., Walters, D., and Thurlow, M.: Assessing a New Coupled Data Assimilation System Based on the Met Office Coupled Atmosphere-Land-Ocean-Sea Ice Model, Monthly Weather Review, 143, 4678–4694, https://doi.org/10.1175/MWR-D-15-0174.1, 2015.

Lüpkes, C., Gryanik, V. M., Hartmann, J., and Andreas, E. L.: A parametrization, based on sea ice morphology, of the neutral atmospheric drag coefficients for weather prediction and climate models, Journal of Geophysical Research: Atmospheres, 117, https://doi.org/10.1029/2012JD017630, http://dx.doi.org/10.1029/2012JD017630, d13112, 2012.

MacLachlan, C., Arribas, A., Peterson, K. A., Maidens, A., Fereday, D., Scaife, A. A., Gordon, M., Vellinga, M., Williams, A., Comer, R. E., Camp, J., Xavier, P., and Madec, G.: Global Seasonal forecast system version 5 (GloSea5): a high-resolution seasonal forecast system, Quarterly Journal of the Royal Meteorological Society, 141, 1072–1084, https://doi.org/10.1002/qj.2396, 2015.

Mahfouf, J.-F., Bergaoui, K., Draper, C., Bouyssel, F., Taillefer, F., and Taseva, L.: A comparison of two off-line soil analysis schemes for assimilation of screen level observations, Journal of Geophysic Research, 114, https://doi.org/10.1029/2008JD011077, 2009.

Masson, V., Le Moigne, P., Martin, E., Faroux, S., Alias, A., Alkama, R., Belamari, S., Barbu, A., Boone, A., Bouyssel, F., Brousseau, P., Brun, E., Calvet, J.-C., Carrer, D., Decharme, B., Delire, C., Donier, S., Essaouini, K., Gibelin, A.-L., Giordani, H., Habets, F., Jidane, M., Kerdraon, G., Kourzeneva, E., Lafaysse, M., Lafont, S., Lebeaupin Brossier, C., Lemonsu, A., Mahfouf, J.-F., Marguinaud, P., Mokhtari, M., Morin, S., Pigeon, G., Salgado, R., Seity, Y., Taillefer, F., Tanguy, G., Tulet, P., Vincendon, B., Vionnet, V., and Voldoire, A.: The SURFEXv7.2 land and ocean surface platform for coupled or offline simulation of earth surface variables and fluxes, Geoscientific Model Development, 6, 929–960, https://doi.org/10.5194/gmd-6-929-2013, http://www.geosci-model-dev.net/6/929/2013/, 2013.

Mélia, D. S.: A global coupled sea ice-ocean model, Ocean Modelling, 4, 137 – 172, https://doi.org/http://dx.doi.org/10.1016/S1463-5003(01)00015-4, http://www.sciencedirect.com/science/article/pii/S1463500301000154, 2002.

Mironov, D. and Ritter, B.: Testing the new ice model for the global NWP system GME of the German Weather Service, Research Activities in Atmospheric and Oceanic Modelling, Rep.34, WMO/TD 1220, 4.21–4.22, 2004.

Mironov, D., Ritter, B., Schulz, J.-P., Buchhold, M., Lange, M., and Machulskaya, E.: Parameterisation of sea and lake ice in numerical weather prediction models of the German Weather Service, Tellus A, 64, 17 330, https://doi.org/10.3402/tellusa.v64i0.17330, 2012.

Mironow, D. and Ritter, B.: First version of the ice model for the global NWP system GME of the German weather service, Research activities in atmospheric and oceanic modelling, Report No. 33, 4.13–4.14, 2003.

Müller, M., Batrak, Y., Kristiansen, J., Køltzow, M. A. O., Noer, G., and Korosov, A.: Characteristics of a Convective-Scale Weather Forecasting System for the European Arctic, Mon. Wea. Rev., 145, 4771–4787, https://doi.org/10.1175/MWR-D-17-0194.1, https://doi.org/10.1175/MWR-D-17-0194.1, 2017.

Müller, M., Homleid, M., Ivarsson, K.-I., Køltzow, M. A. Ø., Lindskog, M., Midtbø, K. H., Andrae, U., Aspelien, T., Berggren, L., Bjørge, D., Dahlgren, P., Kristiansen, J., Randriamampianina, R., Ridal, M., and Vignes, O.: AROME-MetCoOp: A Nordic Convective-Scale Operational Weather Prediction Model, Weather and Forecasting, 32, 609–627, https://doi.org/10.1175/WAF-D-16-0099.1, http://dx.doi.org/10.1175/WAF-D-16-0099.1, 2017.

Parkinson, C. L. and Washington, W. M.: A large-scale numerical model of sea ice, Journal of Geophysical Research: Oceans, 84, 311–337, https://doi.org/10.1029/JC084iC01p00311, http://dx.doi.org/10.1029/JC084iC01p00311, 1979.

Pellerin, P., Ritchie, H., Saucier, F. J., Roy, F., Desjardins, S., Valin, M., and Lee, V.: Impact of a Two-Way Coupling between an Atmospheric and an Ocean-Ice Model over the Gulf of St.Lawrence, Monthly Weather Review, 132, 1379–1398, 2004.

Perovich, D. K.: The Optical Properties of Sea Ice, Tech. Rep. Monograph 96-1, Cold Regions Research and Engineering Lab (CRREL) Hanover NH, U.S. Army Cold Regions Research and Engineering Laboratory 72 Lyme Road Hanover, New Hampshire 03755-1290, http://www.dtic.mil/docs/citations/ADA310586, 1996.

Posey, P. G., Metzeger, E. J., Wallcraft, A. J., Hebert, D. A., Allard, R. A., Smetstad, O. M., Phelps, M. W., Fettere, F., Steward, J. S., Meier, W. N., and Helfrich, S. R.: Improving Arctic sea ice edge forecasts by assimilating high horizonlat resolution sea ice concentration data into the US Navy's ice forecast systems, The Cryosphere, 9, 1735–1745, https://doi.org/10.5194/tc-9-1735-2015, 2015.

Roeckner, E., Arpe, K., Bengtsson, L., Christoph, M., Claussen, M., Dümenil, L., Esch, M., Giorgetta, M., Schlese, U., and Schulzweida, U.: Simulation of the present-day climate with the ECHAM model: Impact of model physics and resolution, Tech. Rep. MPI-Report No. 93, Max Planck Institute for Meteorology, Bundesstrasse 55 D-2000 Hamburg 13 F.R. Germany, http://www.dtic.mil/docs/citations/ADA310586, 1992.

Sakatume, S. and Seki, N.: On the Thermal Properties of Ice and Snow in a Low Temperature Region, Transactions of the Japan Society of Mechanical Engineers, 44, 2059–2069, https://doi.org/10.1299/kikai1938.44.2059, 1978.

Sakov, P., Counillon, F., Bertino, L., Lisæter, K. A., Oke, P. R., and Korablev, A.: TOPAZ4: an ocean-sea ice data assimilation system for the North Atlantic and Arctic, Ocean Science, 8, 633–656, https://doi.org/10.5194/os-8-633-2012, http://www.ocean-sci.net/8/633/2012/, 2012.

Saloranta, T. M.: Modeling the evolution of snow, snow ice and ice in the Baltic Sea, Tellus A, 52, 93–108, https://doi.org/10.1034/j.1600-0870.2000.520107.x, http://dx.doi.org/10.1034/j.1600-0870.2000.520107.x, 2000.

Schwerdtfecer, P.: The Thermal Properties of Sea Ice, Journal of Glaciology, 4, 789–807, https://doi.org/10.1017/S0022143000028379, 1963.

Seity, Y., Brousseau, P., Malardel, S., Hello, G., Bénard, P., Bouttier, F., and Masson, V.: The AROME-France convective-scale operational model, Monthly Weather Review, 139, 976–991, https://doi.org/10.1175/2010MWR3425.1, 2011.

Semmler, T., Cheng, B., Yang, Y., and Rontu, L.: Snow and ice on Bear Lake (Alaska) – sensitivity experiments with two lake ice models, Tellus A: Dynamic Meteorology and Oceanography, 64, 17 339, https://doi.org/10.3402/tellusa.v64i0.17339, http://dx.doi.org/10.3402/tellusa.v64i0.17339, 2012.

Slater, A. G., Schlosser, C. A., Desborough, C. E., Pitman, A. J., Hendersson-Sellers, A., Robock, A., Vinnikov, K. Y., Mitchell, K., Boone, A., Braden, H., Chen, F., Cox, P. M., de Rosnay, P., Dickinson, R. E., Dai, Y.-J., Duan, Q., Entin, J., Etchevers, P., Gedney, N., Gusev, Y. M., Habets, F., Kim, J., Koren, V., Kowalchyk, E. A., Nasonova, O. N., Noilhan, J., Schaake, S., Shmakin, A. B., Smirnova, T. G., Verseghy, D., Wetzel, P., Xue, Y., Yang, Z.-L., and Zeng, Q.: The Representation of Snow in Land Surface Schemes: Results from PILPS 2(d), Journal of Hydrometeorology, 2, 7–25, 2001.

Stark, J., Donlon, C., Martin, M., and McCulloch, M.: OSTIA : An operational, high resolution, real time, global sea surface temperature analysis system, in: OCEANS 2007 - Europe, pp. 1–4, https://doi.org/10.1109/OCEANSE.2007.4302251, 2007.

Thomas, L. H.: Elliptic problems in linear difference equations over a network, Tech. rep., Columbia University, 1949.

Tilling, R. L., Ridout, A., and Shepherd, A.: Near-real-time Arctic sea ice thickness and volume from CryoSat-2, The Cryosphere, 10, 2003–2012, https://doi.org/10.5194/tc-10-2003-2016, 2016.

Tsamados, M., Feltham, D. L., Schroeder, D., Flocco, D., Farrell, S. L., Kurtz, N., Laxon, S. W., and Backon, S.: Impact of Variable Atmospheric and Oceanic Form Drag on Simulations of Arctic Sea Ice, Journal of Physical Oceanography, 44, 1329–1353, https://doi.org/10.1175/JPO-D-13-0215.1, 2014.

Unden, P., Rontu, L., Järvinen, H., Lynch, P., Calvo, J., Cats, G., Cuxart, J., Eerola, K., Fortelius, C., Garcia-Moya, J. A., Jones, C., Geert, Lenderlink, G., Mcdonald, A., Mcgrath, R., Navascues, B., Nielsen, N. W., Degaard, V., Rodriguez, E., Rummukainen, M., Sattler, K., Sass, B. H., Savijarvi, H., Schreur, B. W., Sigg, R., and The, H.: HIRLAM-5 Scientific Documentation, 2002.

Geosci. Model Dev. Discuss., https://doi.org/10.5194/gmd-2018-22
Manuscript under review for journal Geosci. Model Dev.
Discussion started: 20 March 2018

Geoscientific Model Development Discussions
Open Access
EGU

Table 1. Physical parameters of the SICE scheme and parameters for the numerical solution. All the parameters except the ice salinity may be selected by the user, the range and default values are given

Parameter	Value and/or reference
Number of layers in the ice	$[3, 99]$, the default is 4
Number of layers in the snow	the default is 3
Ice thickness	0.75 m
Ice thermal properties	after Schwerdtfecer (1963); Feltham et al. (2006) and Sakatume and Seki (1978)
Ice salinity	3 ppt
Ice albedo	after Perovich (1996) or Parkinson and Washington (1979) or Roeckner et al. (1992)
Radiative transfer within ice	Bouguer-Lambert law, coefficients after Grenfell and Maykut (1977)
Freezing point	the default is -1.8 °C

Geosci. Model Dev. Discuss., https://doi.org/10.5194/gmd-2018-22
Manuscript under review for journal Geosci. Model Dev.
Discussion started: 20 March 2018

Geoscientific Model Development Discussions
Open Access
EGU

Table 2. Design of experiments: Exp. name – the experiment name, Domain – the experiment domain, Length – the length of the experiment run, Ice cover – "fractional" or "binary" for the ice fraction taken into account or not, respectively, Snow scheme – which snow module is used if any, Form drag – whether the parameterization of the form drag used or not.

Exp. name	Domain	Length	Ice cover	Ice scheme	Snow scheme	Form drag
REF	Arctic, MetCoOp	03-04.2013 03.2013	binary	no	no	no
SICE2D-NS	Arctic, MetCoOp	03-04.2013 03.2013	fractional	SICE	no	no
SICE2D-S	Arctic	03-04.2013	fractional	SICE	ISBA ES	no
SICE2D-AD	Arctic	03.2013	fractional	SICE	no	yes

Geosci. Model Dev. Discuss., https://doi.org/10.5194/gmd-2018-22
Manuscript under review for journal Geosci. Model Dev.
Discussion started: 20 March 2018

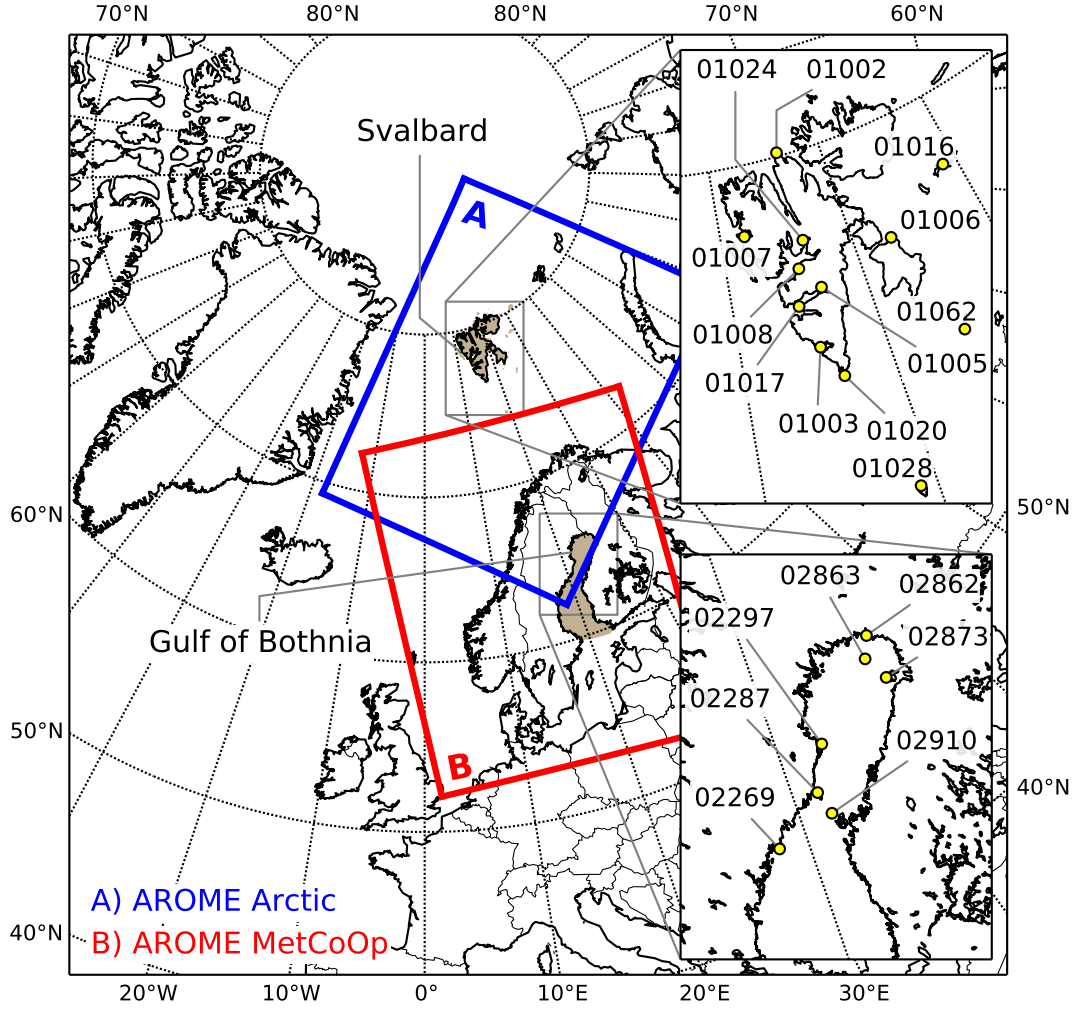

Figure 1. Experiment domains. Insets: locations and WMO numbers of the SYNOP stations at Svalbard and around the Gulf of Bothnia used in this study.

Geosci. Model Dev. Discuss., https://doi.org/10.5194/gmd-2018-22
Manuscript under review for journal Geosci. Model Dev.
Discussion started: 20 March 2018

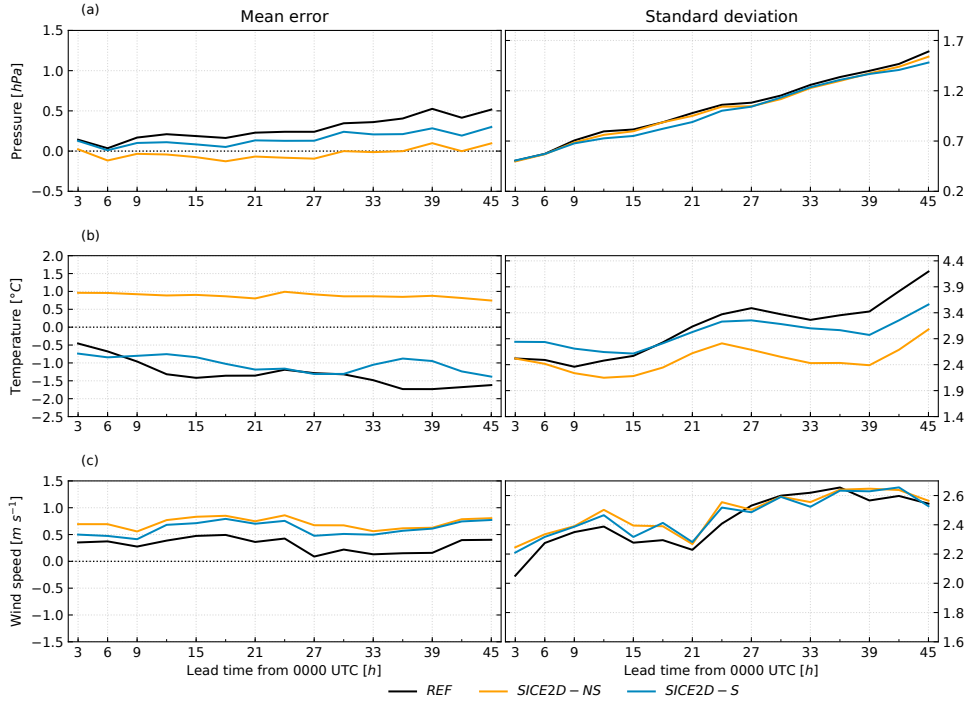

Figure 2. Mean error (left panel) and error standard deviation (right panel) as a function of lead time for forecasts initialized at 0000 UTC for experiments REF, SICE2D-NS and SICE2D-S over the AROME Arctic domain covering the period from 1 March 2013 to 30 April 2013 calculated for 7 Svalbard stations (WMO Nos. 01005, 01006, 01009, 01011, 01016, 01020, 01062). The mean error is calculated as the forecasted value minus observed value. a) mean sea level pressure; b) 2 metre temperature; c) 10 metre wind speed.

Geosci. Model Dev. Discuss., https://doi.org/10.5194/gmd-2018-22
Manuscript under review for journal Geosci. Model Dev.
Discussion started: 20 March 2018

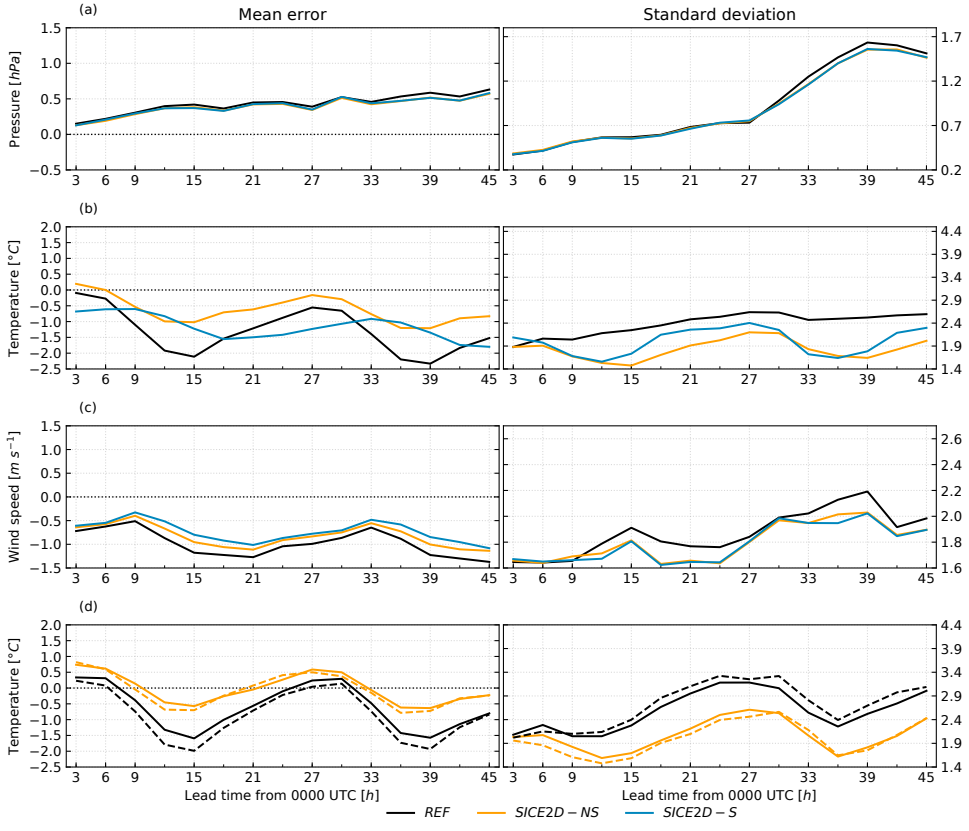

Figure 3. As Fig. 2, but calculated for 7 stations located in the coastal area of the Gulf of Bothnia (WMO Nos. 02269, 02287, 02297, 02862, 02863, 02873, 02910). Figure (d) shows the same error statistics as figure (b) but calculated for all available SYNOP stations located inside the both AROME Arctic (solid lines) and MetCoOp (dashed lines) domains for experiments REF and SICE2D-NS only for March 2013.

Geosci. Model Dev. Discuss., https://doi.org/10.5194/gmd-2018-22
Manuscript under review for journal Geosci. Model Dev.
Discussion started: 20 March 2018

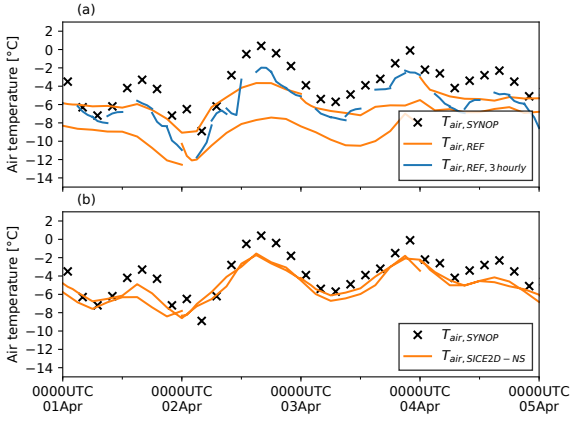

Figure 4. Evolution of the 2 metre temperature for the Kemi I lighthouse station (WMO No. 02863, 65°25' N; 24°08' E), observed (black crosses) and simulated by the 48-h forecasts initialized at 0000 UTC (orange lines) for experiments, a) REF, b) SICE2D-NS. Also in (a), the simulated 2 metre temperature values for the short 3-hour forecasts initialized every 3 hours (except 1200 UTC, which is not shown) that are needed for the initialization of the long forecasts are shown (blue lines).

Geosci. Model Dev. Discuss., https://doi.org/10.5194/gmd-2018-22
Manuscript under review for journal Geosci. Model Dev.
Discussion started: 20 March 2018

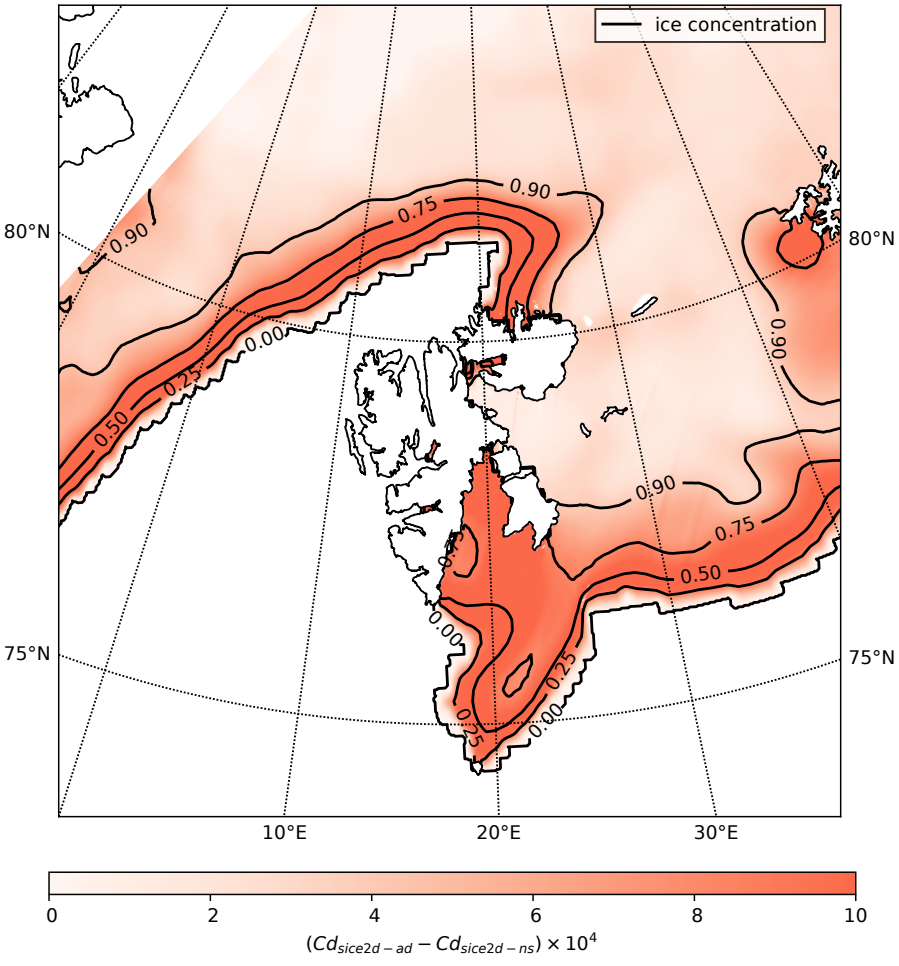

Figure 5. Impact of the form drag term on the average drag coefficient. The shading shows the difference between the average drag coefficients over ice covered areas from the SICE2D-NS and SICE2D-AD experiments for 10 March 2013 0000 UTC. Contours show the ice fraction. Open sea and land points are masked.

Geosci. Model Dev. Discuss., https://doi.org/10.5194/gmd-2018-22
Manuscript under review for journal Geosci. Model Dev.
Discussion started: 20 March 2018

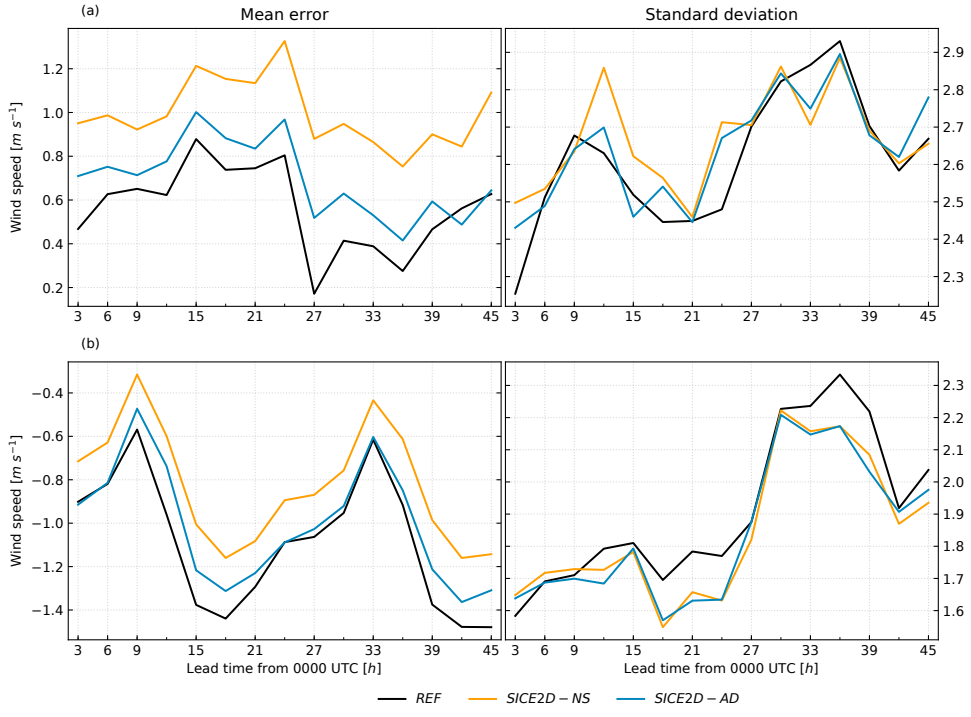

Figure 6. Mean error (left panel) and error standard deviation (right panel) of the 10 metre wind speed as a function of lead time for forecasts initialized at 0000 UTC for experiments REF, SICE2D-NS and SICE2D-AD over the AROME Arctic domain covering the period from 1 March 2013 to 31 March 2013 calculated for: a) 7 Svalbard stations (WMO Nos. 01005, 01006, 01009, 01011, 01016, 01020, 01062), b) 7 stations located in the coastal area of the Gulf of Bothnia (WMO Nos. 02269, 02287, 02297, 02862, 02863, 02873, 02910). The mean error is calculated as the forecasted value minus the observed value.

Geosci. Model Dev. Discuss., https://doi.org/10.5194/gmd-2018-22
Manuscript under review for journal Geosci. Model Dev.
Discussion started: 20 March 2018

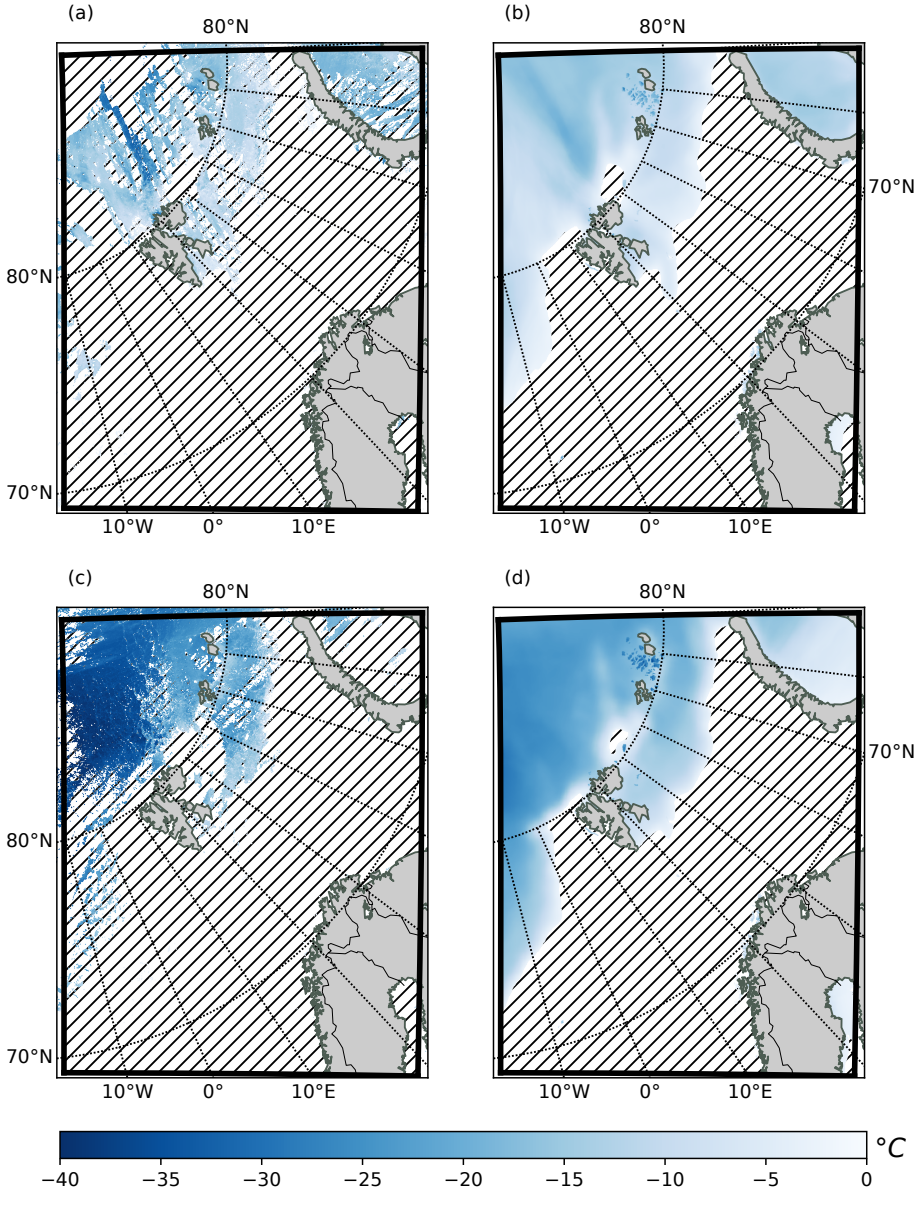

Figure 7. Daily ice surface temperature derived from the MODIS data (left panels) and forecasted by SICE within the HARMONIE-AROME configuration of the ALADIN-HIRLAM NWP system (right panels): a) and b) for 1 March 2017; c) and d) for 9 March 2017. Hatched areas correspond to open sea or missing data.